

Neuroendocrine control of female reproductive function by the activin receptor ALK7

Tatiana Sandoval-Guzmán,^{1,2} Christina Göngrich,² Annalena Moliner, Tingqing Guo, Haiya Wu, Christian Broberger, and Carlos F. Ibáñez³

Department of Neuroscience, Karolinska Institute, Stockholm, Sweden

ABSTRACT Activins are critical components of the signaling network that controls female reproduction. However, their roles in hypothalamus, and the specific functions of their different receptors, have not been elucidated. Here, we investigated the expression and function of the activin receptor ALK7 in the female reproductive axis using *Alk7*-knockout mice. ALK7 was found in subsets of SF1-expressing granulosa cells in the ovary, FSH gonadotrophs in the pituitary, and NPY-expressing neurons in the arcuate nucleus of the hypothalamus. *Alk7*-knockout females showed delayed onset of puberty and abnormal estrous cyclicity, had abnormal diestrous levels of FSH and LH in serum, and their ovaries showed premature depletion of follicles, oocyte degeneration, and impaired responses to exogenous gonadotropins. In the arcuate nucleus, mutant mice showed reduced expression of *Npy* mRNA and lower numbers of *Npy*-expressing neurons than wild-type controls. *Alk7* knockouts showed a selective loss of arcuate NPY/AgRP innervation in the medial preoptic area, a key central regulator of reproduction. These results indicate that ALK7 is an important regulator of female reproductive function and reveal a new role for activin signaling in the control of hypothalamic gene expression and wiring. *Alk7* gene variants may contribute to female reproductive disorders in humans, such as polycystic ovary syndrome.—Sandoval-Guzmán, T., Göngrich, C., Moliner, A., Guo, T., Wu, H., Broberger, C., Ibáñez, C. F. Neuroendocrine control of female reproductive function by the activin receptor ALK7. *FASEB J.* 26, 4966–4976 (2012). www.fasebj.org

Key Words: ovary • pituitary • hypothalamus • NPY • PCOS

Abbreviations: AgRP, agouti gene-related protein; ALK4, activin receptor-like kinase 4; ALK7, activin receptor-like kinase 7; ARC, arcuate nucleus; BAC, bacterial artificial chromosome; CL, corpora lutea; COC, cumulus oocyte complex; EGFP, enhanced green fluorescent protein; FSH, follicle-stimulating hormone; GDF, growth and differentiation factor; GnRH, gonadotropin-releasing hormone; H&E, hematoxylin and eosin; LH, luteinizing hormone; MPOA, medial preoptic area; NPY, neuropeptide Y; P, postnatal day; PB, phosphate buffer; PBS, phosphate-buffered saline; PCOS, polycystic ovary syndrome; PFA, paraformaldehyde; PVN, paraventricular nucleus; SF-1, steroidogenic factor-1; TGF- β , transforming growth factor- β ; V3, third ventricle

THE CONTROL OF REPRODUCTIVE function involves a highly regulated network of hormonal signals exchanged between the gonads, the anterior pituitary, and the brain. The key regulator of reproduction, gonadotropin-releasing hormone (GnRH), is produced by neurons of the medial preoptic area (MPOA) in the hypothalamus, and acts on gonadotrophs in the anterior pituitary to stimulate the synthesis and secretion of luteinizing hormone (LH) and follicle-stimulating hormone (FSH) (1). Circulating LH and FSH stimulate the maturation and development of the gonads and the synthesis and secretion of the gonadal steroid hormones. Among the most important signals regulating reproduction are the activins and inhibins, members of the transforming growth factor- β (TGF- β) superfamily, first described for their ability to respectively stimulate or inhibit secretion of FSH from the anterior pituitary (2, 3). Activins were later found to have effects at different levels of the reproductive axis, including the hypothalamus, pituitary, gonads, and placenta (4–8). In accordance with this, activin and inhibin receptors have been found in reproductive and neuroendocrine tissues from fetal stages to adulthood (9–11).

Similar to other TGF- β superfamily members, activin receptor complexes are formed by type I and type II subunits (12–14). Type I receptors become activated by type II receptors on ligand binding, and are the main signaling output of the receptor complex. The main activin type I receptor, activin receptor-like kinase 4 (ALK4), is ubiquitously expressed (15). Mutant mice lacking ALK4 fail to gastrulate and die at preimplantation stages (16). Although both activin A and B are able to signal through ALK4, only activin B can signal through a second type I receptor, ALK7 (17). ALK7 partners with activin type II receptors A and B to mediate signaling by a subset of TGF- β superfamily ligands, including activin B, nodal, growth and differ-

¹ Present address: DFG Center for Regenerative Therapies Dresden, Technical University of Dresden, Dresden, Germany.

² These authors contributed equally to this work.

³ Correspondence: Department of Neuroscience, Karolinska Institute, Stockholm, Sweden. E-mail: carlos.ibanez@ki.se
doi: 10.1096/fj.11-199059

This article includes supplemental data. Please visit <http://www.fasebj.org> to obtain this information.

entiation factor 1 (GDF1), GDF3, and GDF11 (17–23). Unlike ALK4-knockout mice, mice lacking ALK7 are viable, but display a range of metabolic abnormalities, including increased insulin serum levels, reduced accumulation of white adipose tissue, and partial resistance to high-fat-diet-induced obesity (21, 22, 24). Male mice deficient in activin B phenocopy the insulin phenotype of ALK7 mutants (22) and breed normally (6). On the other hand, female mice lacking activin B have a marked impairment in reproductive function (6). The role of ALK7 in the control of reproduction is unknown.

In the present study, we analyzed the expression of ALK7 along the female reproductive axis, and investigated the role of this receptor in reproductive function in *Alk7*-knockout mice, including effects on the estrous cycle, gonadal development, gonadotropin secretion, and hypothalamic gene expression and wiring. Our results indicate that ALK7 is an important regulator of female reproductive function, acting at multiple levels of the reproductive axis to control the onset of puberty and the female estrous cycle.

MATERIALS AND METHODS

Animals

The generation of *Alk7*-knockout mice has been described previously (24). *InhβB*^{-/-} mice lacking activin B (6) were obtained as frozen embryos from the Jackson Laboratory (stock no. 002442; Jackson Laboratory, Bar Harbor, ME, USA). Both lines were maintained in a C57/BL6 background. Transgenic mice expressing enhanced green fluorescent protein (EGFP) from a bacterial artificial chromosome (BAC) containing the *Alk7* locus (*Alk7*-GFP) were obtained from the GENSAT project (ref. 25; <http://www.gensat.org>). All animals were housed under standard conditions with food and water *ad libitum*. Animal protocols were approved by Stockholm's Norra Djurförsöksetiska Nämnd and in accordance with ethical guidelines of the Karolinska Institute.

Quantitative PCR (qPCR) analysis

On the day of diestrus, brains were removed and placed on a brain matrix to cut 3-mm slices using the optic chiasm as anterior landmark. The hypothalamus was dissected using the end of the optical tract as lateral border and the beginning of the temporal lobe cortex as dorsal border. Pituitaries were also extracted for mRNA studies. The tissue blocks were kept frozen in dry ice until RNA extraction. Total RNA was isolated using a kit (Qiagen, Valencia, CA, USA), according to the manufacturer's protocol. cDNA was synthesized from 600 ng total RNA primed with random hexamers (Invitrogen Life Technologies, Carlsbad, CA, USA) and reverse transcribed with MMLV reverse transcriptase (Invitrogen Life Technologies). Quantitative PCR analysis was performed using the StepOnePlus continuous fluorescence detector (Applied Biosystems Research, Foster City, CA, USA). Product amplification was determined by SYBR Green 1 fluorescence detection. Primers used were *Cga*-upstream, 141–161; *Cga*-downstream, 312–291; *Lhb*-upstream, 37–56; *Lhb*-downstream, 186–166; *Fshb*-upstream, 56–76; *Fshb*-downstream, 167–146; *Npy*-upstream, 222–240; *Npy*-downstream, 270–289; *GnRHR*-up-

stream, 472–491; *GnRHR*-downstream, 565–584; *GnRH*-upstream, 73–93; *GnRH*-downstream, 172–190. Reactions were performed using 2 μl of cDNA, 0.4 μM of forward and reverse primers, and 2× SYBR Green 1 master mix (Applied Biosystems). Standard cycling procedures were employed with annealing temperatures of 60°C. Specific amplicon formation with each primer pair was confirmed by melt curve analysis. Gene expression was quantified relative to standard curves using either TATA box binding protein (TBP) or 18S ribosomal RNA as housekeeping genes. qPCR measurements in hypothalamus were performed in triplicate (samples from 3 animals) and repeated at least twice, often 3 times, with comparable results. In pituitary, 8 animals/group were used in 2 independent experiments.

Antibodies

Antibodies used were as follows: goat anti-GFP (1:500) from Abcam (Cambridge, MA, USA); rabbit anti-FSH (1:500) from AbD Serotec (Kidlington, UK); anti-neuropeptide Y (NPY; 1:200) from Peninsula Labs (Belmont, CA, USA); anti-agouti gene-related protein (AgRP; 1:800) from Millipore (Bedford, MA, USA); anti-goat Alexa Fluor 488 and anti-rabbit Alexa Fluor 555 (1:500–1:1000) from Jackson ImmunoResearch (West Grove, PA, USA) or Invitrogen. According to the manufacturer's information, the anti-FSH antibodies used here do not show cross-reactivity with thyroid-stimulating hormone.

Hormone measurements

Basal FSH and LH secretion were measured in serum obtained from adult females at diestrus, from males, and from peripubertal animals. Serum FSH and LH concentration were measured in a volume of 25 μl using a ELISA kits from Biocode Hycl (Zwölfaxing, Austria) and from Shibayagi (Ishihara, Japan), according to the manufacturer's protocol. Measurements of serum estradiol levels were commissioned to the Endocrine Technology Services Core Laboratory from the Oregon National Primate Research Center (Beaverton, OR, USA).

Estrous cycle analysis

Vaginal smears were taken daily at 2–3 h after lights on, and the cytology was analyzed after Giemsa staining. One estrous cycle was considered the number of days between two proestrous stages (26). Three to four consecutive cycles were analyzed for each animal (11 mice/group). To date the day of first estrus, vaginal smears were taken from the day of vaginal opening.

Ovary histology

Reproductive tracts were dissected and weighed. Ovaries of wild-type and *Alk7*-knockout females were sectioned for morphological analysis and stained with standard hematoxylin and eosin (H&E) protocol. Growing follicles were counted in a single section of the ovary at the widest diameter (wild type, *n*=8; knockout, *n*=9). Staging was performed according to Peters *et al.* (27). For superovulation, 3 wild-type and 3 *Alk7*-knockout females [age postnatal day (P) 26 to P30] were injected i.p. with 5 IU PMS-G at 6 h after lights on on d 1 of treatment, and with 5 IU hCG 48 h later. Wild-type and *Alk7*-knockout control mice received saline injections. At 5 h after the last injection, mice were transcardially perfused with 4% paraformaldehyde (PFA), and their reproductive tracts

were dissected and postfixed. Cryoprotected ovaries were serially sectioned (20 μm) on a cryostat; sections were thaw-mounted to superfrost slides and stained with H&E. The total number of cumulus oocyte complexes (COCs) was determined from serial sections spaced 120 μm apart from each other ($n=3$ mice, 6 ovaries/group).

Pituitary primary culture

Female mice at random estrous stages were anesthetized with isoflurane and killed by cervical dislocation. Pituitaries were collected in Hank's solution with 1 mM HEPES. Anterior lobes were dissociated for 50 min at 36.7°C with 0.3% trypsin. Enzymatic dissociation was stopped with FBS and incubated 5 min with DNase. The cell suspension was centrifuged 6 min at 1100 rpm, and the pellet was resuspended in DMEM for washes. Pellets were resuspended in 2 ml of DMEM without phenol red and supplemented with 2% FBS, penicillin (100 U/ml), and streptomycin (100 $\mu\text{g}/\mu\text{l}$). The dissociated pituitary cells were counted in a hemocytometer and assessed for viability using trypan blue. Only cell preparations with viability >95% were used. Cells were incubated in 48-well dishes in a water-saturated atmosphere, 5% CO_2 and 95% air. After 48 h in culture, cells were washed and preincubated for 6 h with serum-free medium. Medium was changed to DMEM supplemented with 50 ng/ml (1 nM) of recombinant human (rh)-activin A, rh-activin B (R&D Systems), or medium alone. After 24 h, the supernatant was collected and stored at -20°C until processed by ELISA. All incubations were performed in triplicate. Activin concentration and time of incubation were chosen on the basis of previous studies (3). Wells that were used for immunostaining were washed and fixed with 4% PFA prior to immunocytochemistry as described below.

Pituitary immunohistochemistry

Adult female Alk7-GFP mice were transcardially perfused with 4% PFA in phosphate-buffered saline (PBS), and the pituitaries were postfixed overnight at 4°C. Pituitaries cryoprotected in 30% sucrose were coronally sectioned (16 μm) on a cryostat and thaw-mounted on superfrost slides. Blocking, permeabilization, and antibody incubation were carried out in 5% normal donkey serum and 0.2% Triton X-100 in PBS. Primary antibodies were incubated overnight at 4°C, secondary antibodies for 2 h at room temperature. All wash steps were performed with PBS (pH 7.4). Air-dried sections were coverslipped with Dako fluorescence mounting medium (Dako North America, Carpinteria, CA, USA).

Brain immunohistochemistry

At the morning of diestrus, animals were anesthetized with pentobarbital sodium and euthanized by transcardial perfusion with 0.1 M phosphate buffer (PB; pH 7.4) followed by a solution of 4% PFA in PB. The brains were dissected out and postfixed overnight with the same fixative and then cryoprotected with ascending concentration of sucrose at 4°C. The brains were sectioned (12 μm thick), mounted on slides, and stored at -80°C until processed. For immunostaining, sections were rinsed with PBS and blocked with 5% normal serum, 10% BSA, and 0.1% Triton X-100 for 1 h before overnight incubation with primary antibody. Sections were rinsed 3 times with PBS and incubated for 2 h with secondary antibody, then rinsed, and coverslipped with Dako fluorescence mounting medium (Dako North America). Quantification of relative optical density of NPY and AgRP immunoreactivity was performed with ImageJ software (U.S. National Institutes of Health, Bethesda, MD, USA). Sections from 5

wild-type and 5 mutant brains stained with cresyl violet were anatomically matched to Paxinos atlas plate 31 for MPOA, plate 38 for paraventricular nucleus (PVN), and plate 43 for arcuate nucleus (ARC) (28). For GnRH immunohistochemistry, brains were sectioned in the coronal plane on a vibratome (40 μm thick). Antibody incubation was performed in 5% normal donkey serum and 0.2% Triton X-100 at 4°C overnight for primary antibodies and at room temperature for 2 h for secondary antibodies. Nuclei were visualized using DAPI. The number of GnRH-expressing cells was analyzed on every sixth section between bregma +1.94 mm and bregma -2.30 mm.

Colchicine injection

To detect neuropeptides in cell bodies of the ARC of the hypothalamus, axonal transport was blocked using colchicine. Briefly, colchicine was dissolved in 0.9% NaCl to a final concentration of 30 μg in 5 μl . Female mice at diestrus were anesthetized with a mixture of Hypnorm/midazol (1 ml midazolam 5 mg/ml and 1 ml Hypnorm 2.7 ml/kg). Intracerebroventricular injection coordinates were 0.2 mm posterior from bregma, 0.9 mm lateral from midline, and 2 mm deep from brain surface. Colchicine was loaded in a syringe and injected slowly into the right lateral ventricle. To avoid backflow, the needle was left in place for 5 min before removal. Animals were anesthetized 24 h after colchicine injection with an intraperitoneal injection of sodium pentobarbital (0.15 mg/100 g body weight) and perfused *via* the ascending aorta with 25 ml of Tyrode's Ca^{2+} -free solution at 37°C, followed by 25 ml of a mixture of 4% PFA and 0.4% picric acid at 37°C, then perfused with 50 ml of the same mixture at 4°C at a constant flow of 10 ml/min. The brains were dissected and postfixed for 90 min, then rinsed in 10% sucrose/PB (pH 7.4) 3 times and left overnight with several changes in between. The brains were sectioned at 12- μm -thick sections, mounted on slides, and stored at -80°C until processed.

NPY *in situ* hybridization

Females were deeply anesthetized with intraperitoneal pentobarbital sodium, and decapitated in the morning of diestrus. The brain was rapidly dissected out and frozen on dry ice. Fresh frozen coronal sections (14 μm) were mounted on glass slides. Oligonucleotide probes for *Npy* were designed as described previously (29). For stereological analysis of the ARC, sections were chosen according to a mouse brain atlas (28) comprising bregma -1.30 to -1.46 mm. The *in situ* hybridization procedure used has been described previously (29). Antisense probes were labeled with digoxigenin-11-UTP (Roche Diagnostics, Mannheim, Germany). Following 16 h incubation at 42°C, sections were incubated with anti-digoxigenin antibody conjugated with alkaline phosphatase (Boehringer Mannheim, Mannheim, Germany) overnight. Hybridized probes were visualized through a chromogenic reaction with NBT/BCIP (Life Technologies), resulting in a blue-purple precipitate that was examined under bright-field illumination in a Zeiss AxioImager M1 microscope. Cell counts were determined every tenth section at $\times 40$ view within the entire ARC anatomically matched between animals (5 animals/group).

Statistical analysis

To compare data between groups, we used unpaired Student's *t* test or 1-way ANOVA and Tukey's *post hoc* test for data following a normal distribution. Comparison of data not

following a normal distribution was performed using Mann-Whitney *U* test. GraphPad Prism (GraphPad Software, San Diego, CA, USA) and SPSS (IBM, Armonk, NY, USA) were used for data analysis. Values of $P < 0.05$ were considered statistically significant.

RESULTS

ALK7 expression in the reproductive axis

Although earlier studies had reported *Alk7* mRNA expression in ovary, pituitary, and hypothalamus (11, 30–32), the cell types expressing ALK7 within these structures have remained undefined. ALK7-expressing cells were identified by immunostaining for EGFP in a transgenic mouse line expressing EGFP from a BAC encompassing the entire *Alk7* locus (25), which recapitulates endogenous ALK7 expression. In the ovary, ALK7 expression was detected in granulosa cells expressing steroidogenic factor-1 (SF-1; Fig. 1A). In the anterior pituitary, Alk7-GFP expression was detected in FSH-expressing gonadotrophs (Fig. 1B). There is a high overlap between FSH and LH expression in mouse pituitary (33); hence, ALK7 is also expected to be expressed by some LH gonadotrophs. In the hypothalamus, Alk7-GFP expression could be localized to cells immunopositive for NPY in the ARC of colchicine-treated brains (Fig. 1C). Most ($\geq 85\%$) Alk7-GFP cells expressed NPY, but only about half ($51.60 \pm 10.2\%$, $n=5$) of NPY-expressing cells also expressed ALK7. β -Endorphin cells, the second major ascending cell population in the ARC, did not express Alk7-GFP (Fig. 1C, bottom panels). Together, these results indicate that ALK7 is expressed in distinct subpopulations of cells at all levels of the hypothalamic-pituitary-gonadal axis that controls female reproduction.

Delayed puberty onset and abnormal estrous cyclicity in female mice lacking ALK7

Vaginal opening occurs in response to estrogen and is one of the first pubertal markers. There was no significant difference in the onset of vaginal opening between wild-type and *Alk7*-knockout mice (Fig. 2A). Analysis of estradiol serum levels at estrus and diestrus showed no significant difference between the two genotypes (Fig. 2B), although values in the mutant were considerably more variable. After vaginal opening, daily vaginal smears were analyzed from P40 to P60 to assess the day of the first estrus. There was a significant delay in the appearance of the first estrus in *Alk7*-knockout mice (Fig. 2C), indicating a delayed onset of puberty in the absence of ALK7. Detailed analysis of the estrous cycle revealed a significantly lower number of days in estrus and metestrus, as well as longer diestrus in *Alk7*-knockout mice (Fig. 2D). There was also a tendency to longer estrous cycles in the mutants that did not reach statistical significance. Together, these data indicated altered female reproductive function in the absence of ALK7.

Early follicle degeneration, delayed ovulation, and reduced ovulatory competence in ovaries of mice lacking ALK7

Sections of ovaries of P21, P40, and adult mice were analyzed by H&E staining using the follicle classification developed by Peters *et al.* (27) (Fig. 3A). At P21, ovaries of wild-type animals were still compacted, with growing follicles of type 5a, 5b, and 6, along with a few degenerating follicles, as is normal during this stage. Although follicles in stages 5a, 5b, and 6 could also be seen in ovaries of *Alk7*-knockout mice, there were more degenerating follicles without an oocyte, suggesting that degeneration was occurring prematurely in mutant ovaries (Fig. 3A). At P40, ovaries of wild-type animals have a more mature

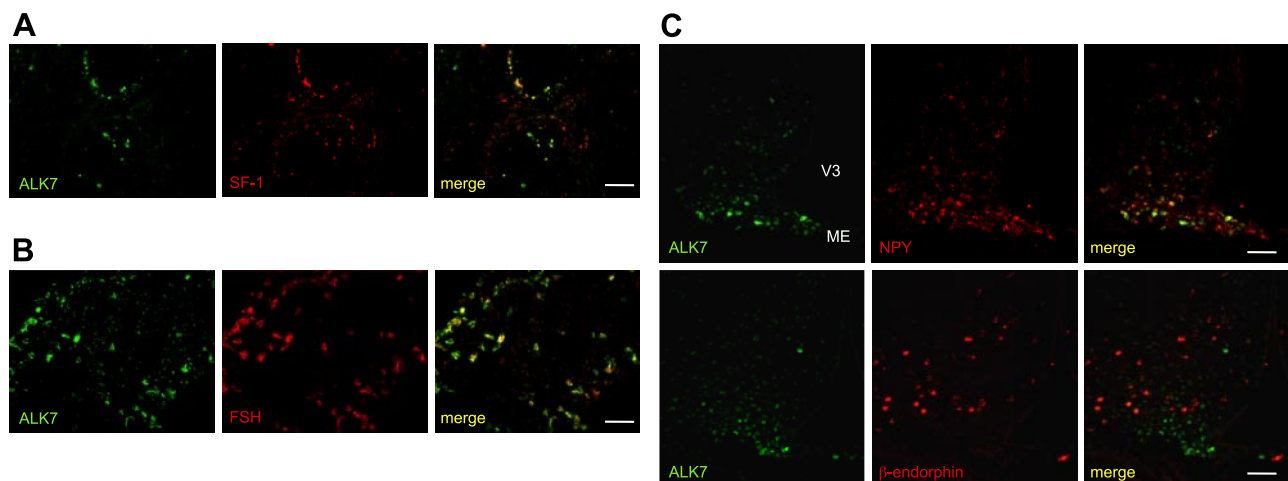


Figure 1. ALK7 expression in the reproductive axis. A) Alk7-GFP immunoreactivity colocalizes with SF-1⁺ cells in adult ovary. B) Alk7-GFP immunoreactivity in adult anterior pituitary colocalizes with FSH. C) Top panels: Alk7-GFP (green) and NPY (red) expression in the ARC of diestrous female mice injected with colchicine. Bottom panels: Alk7-GFP does not colocalize with β -endorphin in the ARC. V3, third ventricle. ME, median eminence. Scale bars = 50 μ m.

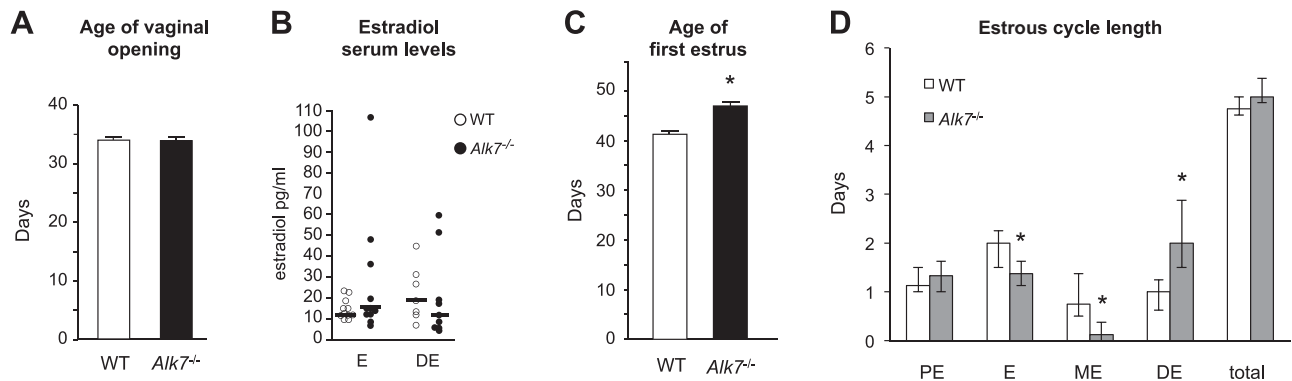


Figure 2. Delayed pubertal onset and abnormal estrous cyclicity in *Alk7*-knockout female mice. **A)** Age of vaginal opening in wild-type (WT) and *Alk7*-knockout (*Alk7*^{-/-}) mice. Results are expressed as means \pm SE ($n=11$). **B)** Estradiol serum levels at estrus (E) and diestrus (DE) in WT and *Alk7*^{-/-} adult mice. Results are expressed as means \pm SE ($n=11$ for measurements at E; $n=7$ WT and $n=9$ *Alk7*^{-/-} for measurements at DE). **C)** Age of first estrus. Results are expressed as means \pm SE (11 animals/group). * $P < 0.05$; 1-way ANOVA and Tukey-Kramer HSD test. **D)** Estrous cycle analysis. Days per cycle in proestrus (PE), estrus (E), metestrus (ME), and diestrus (DE) were counted in 4 consecutive cycles in adult WT and *Alk7*^{-/-} female mice. (One knockout mouse was observed for only 3 cycles because they were too long.) Total cycle length is also indicated. Results are presented as median \pm interquartile range. $P = 0.027$ (E), $P = 0.33$ (ME) and $P = 0.0001$ (DE); Mann-Whitney's *U* test (11 animals/group). * $P < 0.05$.

appearance, with presence of corpora lutea (CL), a sign that ovulation has occurred. In contrast, no CL could be found at P40 in the 5 mutant ovaries examined (Fig. 3A), in agreement with delayed ovulation in females lacking ALK7. At this age, mutant ovaries also displayed higher numbers of degenerating follicles, as in more juvenile stages. At adult stages, ovaries of *Alk7* mutant mice had significantly fewer growing follicles than their wild-type counterparts (7.6 ± 1.3 vs. 13.3 ± 1.2 , $P < 0.05$, $n=8-9$). These data suggest premature depletion of follicles and oocyte degeneration in female mice lacking ALK7. In

contrast, no histological abnormalities could be detected in testis or epididymi of *Alk7*-knockout male mice (Supplemental Fig. S1A).

Ovarian function was investigated in juvenile wild-type and knockout females by induction of superovulation through administration of exogenous gonadotropins (PMSG+hCG). The total number of COCs was determined from serial sections of control and gonadotropin-treated wild type and *Alk7*-mutant mice. COCs were significantly reduced in ovaries from mice lacking ALK7 (Fig. 3B, C), indicating impaired ovulatory competence in the mutants.

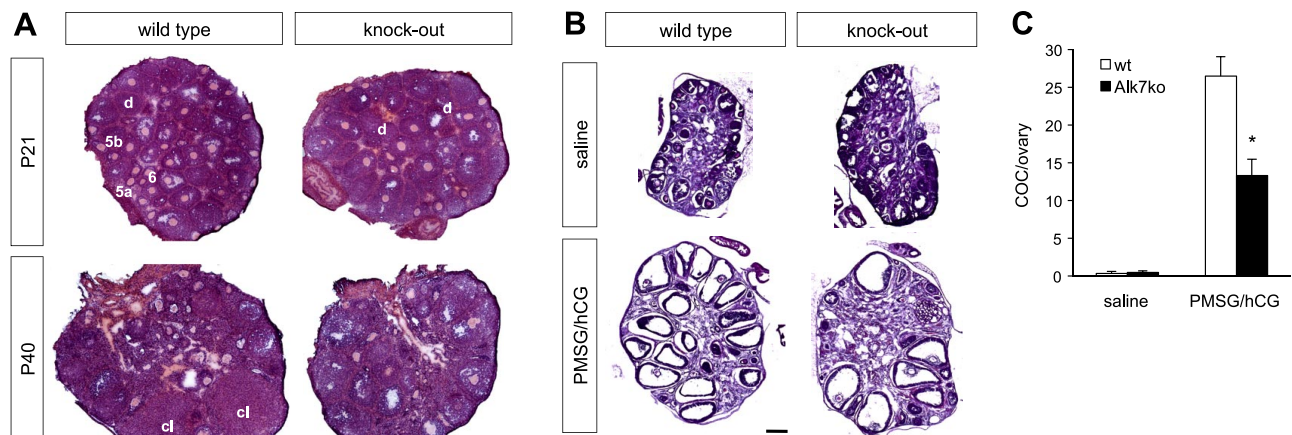


Figure 3. Histological analysis of prepubertal, midpubertal, adult, and superovulated ovaries of wild-type and *Alk7*-knockout mice. **A)** Representative sections of ovaries from P21, P40, and adult wild-type and *Alk7*-knockout mice stained with H&E. Wild-type ovaries have developing follicles of types 5a, 5b, and 6, as well as degenerating follicles (d). In contrast, ovaries from *Alk7*-knockout mice have more degenerating follicles and are more vascularized. Wild-type P40 and adult ovaries already have corpora lutea (CL), a sign that ovulation has occurred.

Ovaries from *Alk7*-knockout females lacked CL. **B)** Analysis of superovulation induced by exogenous administration of gonadotropins (PMSG/hCG) in wild-type and *Alk7*-knockout mice. Representative H&E stainings are shown. Scale bars = 200 μ m (A); 250 μ m (B). **C)** Quantification of COCs after superovulation of wild-type and *Alk7*-knockout mice with PMSG/hCG. Results are shown as average \pm SE COC number per ovary ($n=3$). * $P < 0.05$; Student's *t* test.

Abnormal pituitary function in *Alk7*-knockout mice

To assess pituitary function, we measured the serum concentration of FSH in prepuberty (P21), midpuberty (P40), and adult animals. Although somewhat higher than normal at prepuberty, serum FSH levels were found to decline with age in mutant females, and they were significantly lower than in wild-type animals at both midpubertal and adult (diestrus) stages (Fig. 4A). Serum FSH levels were normal in adult males lacking ALK7 (Supplemental Fig. S1B). On the other hand, LH levels in serum were higher in adult *Alk7* mutant females than in wild-type controls at diestrus (Fig. 4B). It has been previously reported that deletion of the *Fshβ* gene results in elevated LH levels in mice (34). At the mRNA level, a modest increase in *Lhbeta* mRNA was detected by quantitative PCR in the pituitary from mice lacking ALK7 (Fig. 4C). No change was found in either *Cga* or *Fshβ* mRNA levels between wild-type and mutant pituitary (Fig. 4C). Next, we assessed secretion of FSH and LH in cultures of pituitary cells dissociated from the adult pituitary. As in the intact gland, a proportion of FSH gonadotrophs also expressed ALK7 in culture (Fig. 4D). However, there was no difference in either basal or activin-stimulated FSH secretion between wild-type and *Alk7*-mutant pituitary cells (Fig. 4E). On the other hand, basal LH secretion was higher in cultures

derived from mutant pituitary (Fig. 4E), in concordance with the *in vivo* results. Together, these results indicated an increased LH/FSH ratio in serum of *Alk7*-mutant female mice and LH hypersecretion by pituitary cells lacking ALK7.

Reduced *Npy* expression and *Npy* neuron number in the ARC of *Alk7*-knockout mice

Given the overlap between ALK7 and NPY expression in neurons of the ARC of the hypothalamus (Fig. 1C) and the important roles played by arcuate NPY neurons in the control of female reproduction, we investigated whether lack of ALK7 had any effect on *Npy* mRNA expression and *Npy* neuron number in the arcuate. qPCR analysis revealed that levels of *Npy* mRNA were significantly reduced (by ~40%) in the ARC of *Alk7*-knockout female mice (Fig. 5A). Interestingly, mutant mice lacking activin B (*Inhbb*^{-/-}) also showed reduced *Npy* mRNA expression in the ARC (Fig. 5A), raising the possibility that activin B acts through ALK7 to positively regulate *Npy* mRNA expression or *Npy* neuron number in this nucleus. To address this latter possibility, we analyzed the distribution of neurons expressing *Npy* mRNA in the ARC by *in situ* hybridization (Fig. 5B). Eight anatomically matched sections from wild-type and mutant animals (4 animals/group) were analyzed,

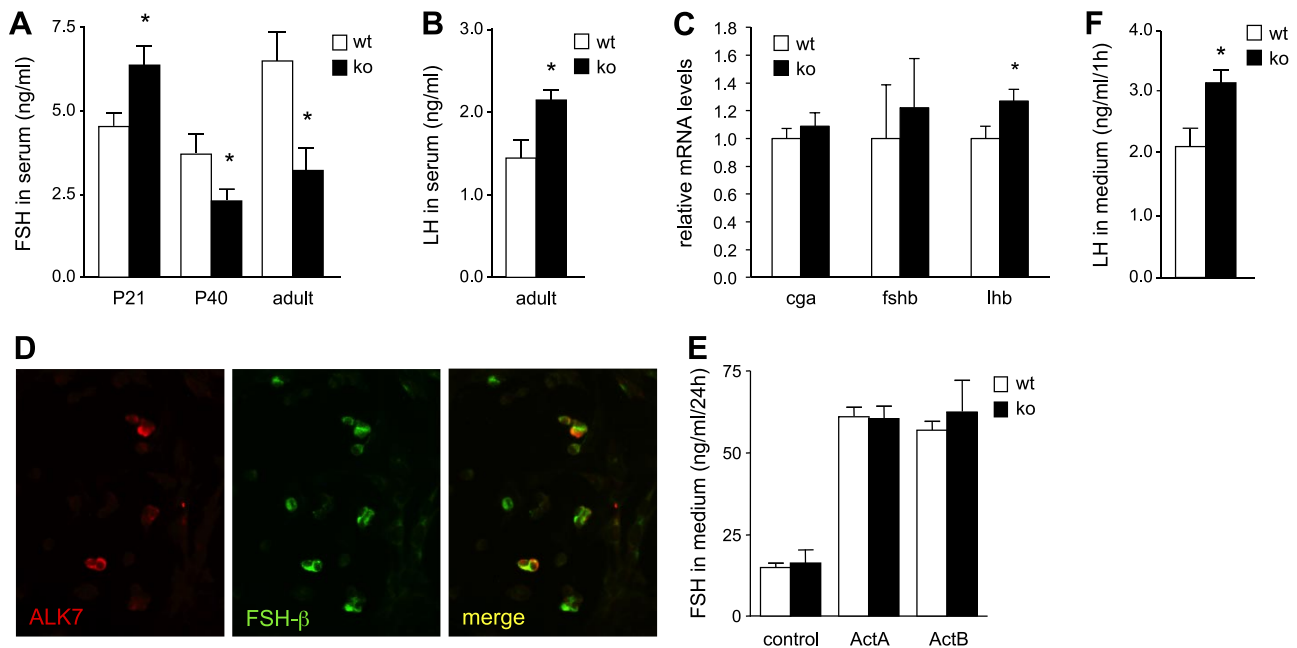


Figure 4. Basal FSH secretion in serum and dissociated pituitary cells from wild-type (wt) and *Alk7*-knockout (ko) mice. **A)** Basal levels of FSH in serum of prepubertal (P21), midpubertal (P40), and adult females (on the morning of diestrus) as detected by ELISA. FSH concentration is expressed in nanograms per milliliter. Data are expressed as means \pm SE (10 animals/group). * $P < 0.05$; Student's *t* test. **B)** Basal serum levels of LH in adult females (diestrus) as detected by ELISA. Data are expressed as means \pm SE (10 animals/group). * $P < 0.05$; Student's *t* test. **C)** Analysis of *Cga*, *Fshβ*, and *Lhb* mRNA levels in pituitaries of adult wild-type and *Alk7*-knockout mice by quantitative PCR. Data are expressed as means \pm SE (8 animals/group). * $P = 0.04$; Student's *t* test. **D)** ALK7 immunoreactivity in primary cultures of pituitary cells. All ALK7-expressing cells are also positive for FSH, identifying them as gonadotrophs. Not all FSH⁺ cells express ALK7. Scale bar = 20 μ m. **E)** Pituitary primary cultures were stimulated with 50 ng/ml (1 nM) of activin A (ActA), activin B (ActB), or medium for 24 h. Supernatant was collected to quantify secretion of FSH by ELISA. Data are expressed as means \pm SE collected from 3 separate experiments. **F)** Supernatant of pituitary primary cultures (1 h) was collected to quantify basal LH secretion by ELISA. Data are expressed as means \pm SE ($n=5$). * $P < 0.05$; Student's *t* test.

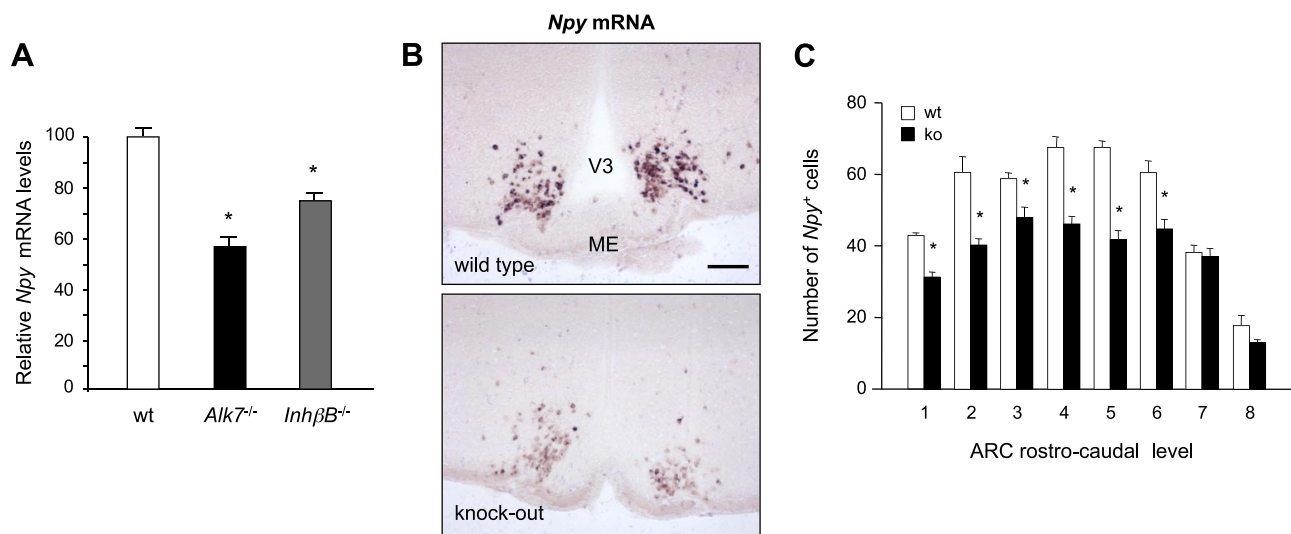


Figure 5. Reduced *NPY* mRNA expression and loss of *NPY*⁺ neurons in the ARC of *Alk7*-knockout mice. **A)** Relative *NPY* mRNA expression in hypothalamus of diestrous wild-type (wt), *Alk7*-knockout (*Alk7*^{-/-}), and *InhβB*-knockout (*InhβB*^{-/-}) adult females, as quantified by qPCR. Relative units were obtained after normalization to TATA binding protein expression and are expressed as fold increase relative to wild type. Results represent means ± SE of triplicate determinations (3 animals/group). **P* < 0.05; Student's *t* test. **B)** *Npy* mRNA expression in coronal sections through the ARC of wild-type and *Alk7*-knockout animals detected by *in situ* hybridization. ME, median eminence; V3, third ventricle. Scale bar = 100 μm. **C)** Mean *NPY* cell number across anatomically matched sections of the ARC in wild-type (wt) and *Alk7*-knockout (ko) animals. Quantification was done in matched sections from every tenth section from each brain (5 animals/group). **P* < 0.005; Student's *t* test.

and cells positive for *Npy* mRNA expression were counted. The highest cell count was observed in the central region of the nucleus in both groups. Interestingly, the anterior and medial regions of the arcuate from *Alk7*-knockout mice showed a significant loss of cells expressing *Npy* mRNA (Fig. 5C). Overall, *Alk7*^{-/-} female mice showed a 27 ± 2.3% reduction in the number of *Npy* neurons in the ARC compared to wild-type controls.

Reduced *NPY* and *AgRP* innervation of hypothalamic medial preoptic area in mice lacking *ALK7*

NPY fibers originating in the ARC project anteriorly to the PVN and to the MPOA of the hypothalamus. *NPY* innervation of the MPOA plays an important role in regulating the production and release of *GnRH* (35–37). We investigated whether the absence of *ALK7* affected the *NPY* projection from the arcuate to these nuclei by immunohistological labeling of *NPY* fibers in brain sections of wild-type and *Alk7*-knockout mice. In the PVN, there was a normal complement of *NPY* fibers in sections of the *Alk7* knockout (Fig. 6A, C). In contrast, the density of *NPY* fibers was greatly reduced (by ~70%) in the dorsal aspect of the MPOA in the mutants (Fig. 6B, C), suggesting a selective deficiency in *NPY* innervation of this target of the arcuate. *AgRP* is exclusively expressed by arcuate *NPY* neurons and has been used as a specific marker of *NPY* projections from the arcuate (29). To assess whether the paucity of *NPY* fibers in the mutant MPOA was indeed due to a deficit in the projection from the arcuate, immunohistochemistry for *AgRP* was performed in the MPOA of wild-type

and *Alk7*-mutant female mice (Fig. 6D). *AgRP* fiber density was found to be reduced by 40% in the MPOA of the mutants (Fig. 6E), indicating that the *NPY/AgRP* projection from the arcuate to the MPOA is abnormal in *Alk7*-knockout mice. No difference was found in the number of neurons expressing *GnRH* (80.8 ± 23.2 vs. 76.0 ± 18.2 *GnRH* cells; *n* = 5; *P* = 0.97) or in *GnRH* mRNA levels (data not shown) in the MPOA of female mice lacking *ALK7* compared to wild types.

DISCUSSION

The control of female reproduction is accomplished by a complex network of feedforward and feedback regulatory interactions between the gonads, the pituitary, and the hypothalamus. Activins play crucial roles in this network at different levels of the reproductive axis and have been widely studied for >2 decades. Although their expression and function in ovary and pituitary gland have been well documented, their actions on central hypothalamic nuclei are not well understood. Because of the embryonic lethality of mice lacking *ALK4*, elucidation of the specific role of this activin receptor in reproduction awaits the generation and analysis of conditional mutants. The second type I activin receptor, *ALK7*, binds activin B but not activin A, in addition to other ligands of the TGF-β superfamily. Mutant mice lacking *ALK7* are viable and, in this study, we report the first characterization of the reproductive axis of mice lacking this receptor.

In agreement with the phenotype of mice lacking

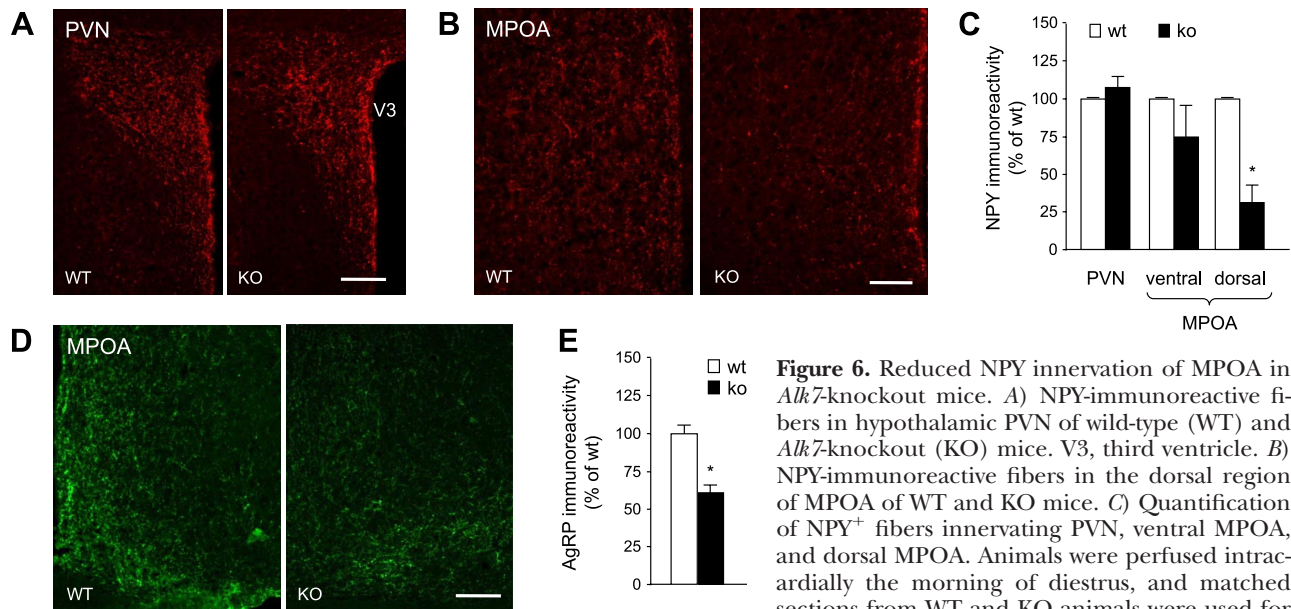


Figure 6. Reduced NPY innervation of MPOA in *Alk7*-knockout mice. *A*) NPY-immunoreactive fibers in hypothalamic PVN of wild-type (WT) and *Alk7*-knockout (KO) mice. V3, third ventricle. *B*) NPY-immunoreactive fibers in the dorsal region of MPOA of WT and KO mice. *C*) Quantification of NPY⁺ fibers innervating PVN, ventral MPOA, and dorsal MPOA. Animals were perfused intracardially the morning of diestrus, and matched sections from WT and KO animals were used for analysis. Data are presented as means \pm SE ($n=5$). * $P < 0.05$, Student's *t* test. *D*) AgRP-immunoreactive fibers in the MPOA of WT and KO mice. Scale bars = 100 μ m (*A*, *D*); 50 μ m (*C*). *E*) Quantification of AgRP⁺ fibers innervating the MPOA. Data are presented as means \pm SE ($n=5$). * $P < 0.05$; Student's *t* test.

activin B, female (but not male) mice lacking the ALK7 receptor displayed reproductive function defects. However, the abnormalities observed in *Alk7*-knockout females were of a different character, suggesting different roles for the ALK7 and ALK4 receptors in mediating the actions of activin B during reproduction control. Activins are expressed throughout ovarian development (9) and contribute to the formation of the initial follicle pool (38). Activins are also important regulators of follicle growth in mature ovaries (39). Our results suggest that ALK7 may mediate some of the effects of activin B, the most abundant activin in developing ovary, on follicular pool maintenance at puberty, the time when massive degradation occurs and developmental competence is acquired. In the mature ovary, ALK7 was expressed in SF-1⁺ granulosa cells. As these cells also express activin subunits (39), this finding supports an autocrine/paracrine mode of action for activin B in ovary (39, 40). As activin B, unlike activin A, is constantly expressed during the cycle (39, 41), our results suggest that activin B signaling through ALK7 has a tonic role in adult ovary homeostasis, rather than in promoting ovulation. Two previous *in vitro* studies using overexpression of a constitutively active ALK7 mutant in an epithelial ovarian cancer cell line (42) or in cultures of dissociated granulosa cells (43) reported that this receptor mediated antiproliferative and apoptotic effects of Nodal in ovarian cells. However, the ovaries of adult mice lacking ALK7 did not show any signs of hypertrophy, cyst incidence, or tumor formation, suggesting that ALK7 does not have a proapoptotic function *in vivo*. On the contrary, the paucity of growing follicles and CL in ovaries of *Alk7*-knockout females resemble the phenotype of transgenic mice overexpressing the inhibin α subunit, which is known to oppose several of the functions of activins (44),

suggesting that ALK7 contributes to establish the physiological balance between activins and inhibins in the ovary. A direct role of ALK7 in ovarian function was confirmed by the reduced superovulation observed in *Alk7*-knockout females following treatment with exogenous gonadotropins, indicating reduced ovarian competence in the mutants. Estrogen and testosterone are known to exert very different effects on several components of the activin signaling pathway, including expression of activin B, Smad2, Smad3, Smad7, and the endogenous activin inhibitor follistatin (45). They are also thought to regulate FSH production, in part, through the activin signaling system. It is possible that the different actions of female and male steroids on the activin signaling system underlie the dimorphic effects of the *Alk7* mutation on reproductive function.

In addition to cell-autonomous defects in the ovaries of mice lacking ALK7, our results also point to abnormal gonadotropin levels as one of the primary abnormalities underlying the reduced fertility of females lacking ALK7. LH hypersecretion by mutant pituitary cells correlated with higher LH serum levels in *Alk7*-knockout females, suggesting a defect in mutant gonadotrophs. On the other hand, mice lacking ALK7 showed significantly reduced FSH levels at puberty and adult stages compared to wild-type controls. Reduced FSH production, as in mice deficient in FSH- β subunit, has been shown to result in increased serum LH levels (34). Although pituitary derived activin B contributes to the tonic, autocrine regulation of basal FSH secretion by gonadotrophs (8, 46–48), we found that neither basal nor activin-stimulated FSH secretion from pituitary cultures of *Alk7*-knockout mice was different from wild-type mice, suggesting that the ALK4 receptor, which can bind both activins and is also present in gonadotrophs, can compensate for the lack of ALK7 in

these cells. *In vivo* FSH levels are regulated by complex feedback and feedforward systems involving the action of steroids, gonadotropins, GnRH, and activins/inhibins on ovaries, pituitary, and hypothalamus. As shown here, ALK7 is not only expressed in pituitary, but also hypothalamus and ovary, and so it is likely that the combined loss of ALK7 signaling in those tissues underlies the apparent discrepancy between the *in vivo* and *in vitro* effects of ALK7 loss on FSH levels.

ALK7 was localized to NPY-expressing neurons in the ARC. In this structure, mutant mice lacking ALK7 showed reduced expression of *Npy* mRNA and lower numbers of *Npy*-expressing neurons compared to wild-type controls. In addition, a similar reduction in *Npy* mRNA expression was also observed in *InhβB*-knockout animals, lacking the ALK7 ligand activin B. Together, these data suggest that activin B signaling through ALK7 functions cell-autonomously to regulate *Npy* mRNA expression and/or *Npy* neuron number in the ARC. It should also be noted that insulin can reduce arcuate *Npy* transcription following central administration (49). Because both *Alk7*- and *InhβB*-mutant mice have increased serum insulin levels, it is also possible that this contributes to the reduced levels of *Npy* expression in the ARC of these mutants. At this point, it is unclear whether a subset of *Npy*-expressing neurons is lost in *Alk7* mutants or has simply down-regulated *Npy* expression to undetectable levels. In any case, it is clear that less NPY is being made in the arcuate of *Alk7*-knockout animals.

The arcuate NPY system provides direct input to GnRH cell bodies of the MPOA (50–52), where it contributes to the regulation of GnRH secretion (37, 53). Interestingly, NPY fiber density was drastically reduced in the dorsal MPOA of mutants lacking ALK7. Although the MPOA is thought to receive NPY innervation from other structures (*i.e.*, brain stem) in addition to the ARC (52), the parallel reduction in AgRP⁺ fibers, all of which originate from NPY arcuate neurons (54, 55), indicates impaired arcuate NPY/AgRP innervation of GnRH neurons in *Alk7*-knockout mutants. Reduced NPY/AgRP innervation of the MPOA is expected to affect the pulsatile release of GnRH at the median eminence (36, 36, 37, 37, 53, 53, 56). In this regard, it should be noted that, although NPY has generally been proposed to have a stimulatory effect on LH secretion, deletion of the *Npy* gene has been shown to attenuate the preovulatory LH surge but to have little effect on basal LH levels at metestrus (57). *Alk7*-mutant mice have lost 27% of arcuate NPY neurons, but not all, and it is possible that an imbalance in MPOA innervation leads to abnormal GnRH stimulation of pituitary gonadotrophs and regulation of FSH/LH secretion.

In contrast to the MPOA, no reduction in NPY fiber density was observed in the mutant PVN, a second major rostral target of arcuate NPY fibers (29, 58). This indicates that the NPY deficits observed in the ARC of mice lacking ALK7 did not propagate across all arcuate NPY projections. The selective loss of arcuate NPY/AgRP fibers in the MPOA suggests that ALK7 plays a

distinct role in hypothalamic wiring in addition to regulation of arcuate *Npy* mRNA levels and neuron number. Notably, ALK7 is not expressed in either MPOA or PVN (data not shown). The loss of NPY/AgRP fibers in the MPOA could thus be explained by a selective dependence of a subpopulation of MPOA-projecting arcuate NPY neurons on ALK7. There is evidence supporting neurotrophic functions of activins as stimulators of both synaptic connectivity (59) and neuronal survival (60). It is currently unclear whether different subsets of arcuate NPY neurons project to MPOA and PVN or whether the same neurons send collaterals that terminate in both targets. It is, therefore, possible that ALK7 regulates the differential innervation of these nuclei by the arcuate by, for example, mediating neurotrophic functions of MPOA-derived activins. The study of mice lacking ALK7 opens an opportunity to address several fundamental questions about hypothalamic connectivity.

We note that female mice lacking ALK7 show several of the abnormalities found in patients with the human condition known as polycystic ovary syndrome (PCOS), including abnormal estrous cyclicity, ovulatory dysfunction, LH hypersecretion, increased LH/FSH ratio, hyperinsulinemia, and insulin resistance (22, 61). Genetic factors are known to influence the development of PCOS, and several gene variants have been found to be associated with this syndrome. A variant that has been consistently replicated in different studies is present in the gene encoding the human Activin type IIA receptor (61, 62), indicating that abnormal activin signaling may contribute to PCOS. No single gene variant is expected to account for all the features of PCOS, and it is, therefore, not surprising that ALK7-mutant mice phenotype only some of the abnormalities found in this syndrome. On the basis of our results, we suggest that gene variants in *Acvr1c* (the locus encoding ALK7) may represent risk factors for human PCOS.

In summary, our results indicate that ALK7 is a crucial regulator of female reproductive function and reveal a new role for activin signaling in the control of hypothalamic gene expression and wiring. **FJ**

This work was supported by grants from the Swedish Research Council, the Swedish Cancer Society, and the European Research Council to C.F.I.; and the Swedish Research Council, Novo Nordisk Foundation, and European Research Council to C.B.

REFERENCES

1. Matsuo, H., Baba, Y., Nair, R. M., Arimura, A., and Schally, A. V. (1971) Structure of the porcine LH- and FSH-releasing hormone. I. The proposed amino acid sequence. *Biochem. Biophys. Res. Commun.* **43**, 1334–1339
2. Vale, W., Rivier, C., Hsueh, A., Campen, C., Meunier, H., Bicsak, T., Vaughan, J., Corrigan, A. Z., Bardin, W., and Sawchenko, P. (1988) Chemical and biological characterization of the inhibin family of protein hormones. *Recent Progr. Hormone Res.* **44**, 1–34
3. Bilezikjian, L. M. (1993) Activin-A regulates follistatin secretion from cultured rat anterior pituitary cells. *Endocrinology* **133**, 2554–2560

4. Furuta, C., Arakawa, S., Shi, Z., Watanabe, G., and Taya, K. (2008) Placental activin A is required for follicular development during the second half of pregnancy in the golden hamster (*Mesocricetus auratus*). *Endocrine* **33**, 126–134
5. Plotsky, P. M., Kjaer, A., Sutton, S. W., Sawchenko, P. E., and Vale, W. (1991) Central activin administration modulates corticotropin-releasing hormone and adrenocorticotropin secretion. *Endocrinology* **128**, 2520–2525
6. Vassalli, A., Matzuk, M. M., Gardner, H. A., Lee, K.-F., and Jaenisch, R. (1994) Activin/inhibin beta B subunit gene disruption leads to defects in eyelid development and female reproduction. *Genes Dev.* **8**, 414–427
7. Calogero, A. E., Burrello, N., Ossino, A. M., Polosa, P., and D'Agata, R. (1998) Activin-A stimulates hypothalamic gonadotropin-releasing hormone release by the explanted male rat hypothalamus: interaction with inhibin and androgens. *J. Endocrinol.* **156**, 269–274
8. González-Manchón, C., Bilezikjian, L. M., Corrigan, A. Z., Mellon, P. L., and Vale, W. (1991) Activin-A modulates gonadotropin-releasing hormone secretion from a gonadotropin-releasing hormone-secreting neuronal cell line. *Neuroendocrinology* **54**, 373–377
9. Weng, Q., Wang, H. S. M., edan, M., Jin, W., Xia, G., Watanabe, G., and Taya, K. (2006) Expression of inhibin/activin subunits in the ovaries of fetal and neonatal mice. *J. Reprod. Dev.* **52**, 607–616
10. Wilson, M. E., and Handa, R. J. (1998) Activin subunit, follistatin, and activin receptor gene expression in the prepubertal female rat pituitary. *Biol. Reprod.* **59**, 278–283
11. Rydén, M., Imamura, T., Jörnvall, H., Belluardo, N., Neveu, I., Trupp, M., Okadome, T., Dijke, ten, P., and Ibanez, C. F. (1996) A novel type I receptor serine-threonine kinase predominantly expressed in the adult central nervous system. *J. Biol. Chem.* **271**, 30603–30609
12. Shi, Y., and Massagué, J. (2003) Mechanisms of TGF- β signaling from cell membrane to the nucleus. *Cell* **113**, 685–700
13. Derynck, R., Akhurst, R. J., and Balmain, A. (2001) TGF- β signaling in tumor suppression and cancer progression. *Nat. Genet.* **29**, 117–129
14. ten Dijke, P., Miyazono, K., and Heldin, C.-H. (2000) Signaling inputs converge on nuclear effectors in TGF- β signaling. *Trends Biochem. Sci.* **25**, 64–70
15. Attisano, L., Cárcamo, J., Ventura, F., Weis, F. M., Massagué, J., and Wrana, J. L. (1993) Identification of human activin and TGF- β type I receptors that form heteromeric kinase complexes with type II receptors. *Cell* **75**, 671–680
16. Gu, Z., Nomura, M., Simpson, B. B., Lei, H., Feijen, A., van den Eijnden-van Raaij, A., Donahoe, P. K., and Li, E. (1998) The type I activin receptor ActRIB is required for egg cylinder organization and gastrulation in the mouse. *Genes Dev.* **12**, 844–857
17. Tsuchida, K., Nakatani, M., Yamakawa, N., Hashimoto, O., Hasegawa, Y., and Sugino, H. (2004) Activin isoforms signal through type I receptor serine/threonine kinase ALK7. *Mol. Cell. Endocrinol.* **220**, 59–65
18. Andersson, O., Bertolino, P., and Ibanez, C. F. (2007) Distinct and cooperative roles of mammalian Vg1 homologs GDF1 and GDF3 during early embryonic development. *Dev. Biol.* **311**, 500–511
19. Andersson, O., Reissmann, E., and Ibanez, C. F. (2006) Growth differentiation factor 11 signals through the transforming growth factor- β receptor ALK5 to regionalize the anterior-posterior axis. *EMBO Rep.* **7**, 831–837
20. Andersson, O., Reissmann, E., Jörnvall, H., and Ibanez, C. F. (2006) Synergistic interaction between Gdf1 and Nodal during anterior axis development. *Dev. Biol.* **293**, 370–381
21. Andersson, O., Korach-Andre, M., Reissmann, E., Ibanez, C. F., and Bertolino, P. (2008) Growth/differentiation factor 3 signals through ALK7 and regulates accumulation of adipose tissue and diet-induced obesity. *Proc. Natl. Acad. Sci. U. S. A.* **105**, 7252–7256
22. Bertolino, P., Holmberg, R., Reissmann, E., Andersson, O., Berggren, P.-O., and Ibanez, C. F. (2008) Activin B receptor ALK7 is a negative regulator of pancreatic beta-cell function. *Proc. Natl. Acad. Sci. U. S. A.* **105**, 7246–7251
23. Reissmann, E., Jörnvall, H., Blokzijl, A., Andersson, O., Chang, C., Minchiotti, G., Persico, M. G., Ibanez, C. F., and Hemmati-Brivanlou, A. H. (2001) The orphan receptor ALK7 and the activin receptor ALK4 mediate signaling by Nodal proteins during vertebrate development. *Genes Dev.* **15**, 2010–2022
24. Jörnvall, H., Reissmann, E., Andersson, O., Mehrkash, M., and Ibanez, C. F. (2004) ALK7, a receptor for nodal, is dispensable for embryogenesis and left-right patterning in the mouse. *Mol. Cell. Biol.* **24**, 9383–9389
25. Gong, S., Zheng, C., Doughty, M. L., Losos, K., Didkovsky, N., Schambra, U. B., Nowak, N. J., Joyner, A., Leblanc, G., Hatten, M. E., and Heintz, N. (2003) A gene expression atlas of the central nervous system based on bacterial artificial chromosomes. *Nature* **425**, 917–925
26. Goldman, J. M., Murr, A. S., and Cooper, R. L. (2007) The rodent estrous cycle: characterization of vaginal cytology and its utility in toxicological studies. *Birth Defects Res. B Dev. Reprod. Toxicol.* **80**, 84–97
27. Peters, H. (1969) The development of the mouse ovary from birth to maturity. *Acta Endocrinol.* **62**, 98–116
28. Paxinos, G., and Franklin, K. B. J. (2004) *The Mouse Brain in Stereotaxic Coordinates*, 2nd Ed., Gulf Publishing, Houston, TX, USA
29. Broberger, C., Johansen, J., Johansson, C., Schalling, M., and Hökfelt, T. (1998) The neuropeptide Y/agouti gene-related protein (AGRP) brain circuitry in normal, anorectic, and monosodium glutamate-treated mice. *Proc. Natl. Acad. Sci. U. S. A.* **95**, 15043–15048
30. Bondestam, J., Huotari, M. A., Morén, A., Ustinov, J., Kaivo-Oja, N., Kallio, J., Horelli-Kuitunen, N., Aaltonen, J., Fujii, M., Moustakas, A., ten Dijke, P., Otonkoski, T., and Ritvos, O. (2001) cDNA cloning, expression studies and chromosome mapping of human type I serine/threonine kinase receptor ALK7 (ACVR1C). *Cytogenet. Cell Genet.* **95**, 157–162
31. Lorentzon, M., Hoffer, B. J., Ebendal, T., Olson, L., and Tomac, A. C. (1996) Habrec1, a novel serine/threonine kinase TGF- β type I-like receptor, has a specific cellular expression suggesting function in the developing organism and adult brain. *Exp. Neurol.* **142**, 351–360
32. Bernard, D. J., Lee, K. B., and Santos, M. M. (2006) Activin B can signal through both ALK4 and ALK7 in gonadotrope cells. *Reprod. Biol. Endocrinol.* **4**, 52
33. Nakane, P. K. (1970) *Classifications of anterior pituitary cell types with immunoenzyme histochemistry.* **18**, 9–20
34. Kumar, T. R., Wang, Y., Lu, N., and Matzuk, M. M. (1997) Follicle-stimulating hormone is required for ovarian follicle maturation but not male fertility. *Nat. Genet.* **15**, 201–204
35. Crowley, W. R., and Kalra, S. P. (1987) Neuropeptide Y stimulates the release of luteinizing hormone-releasing hormone from medial basal hypothalamus in vitro: modulation by ovarian hormones. *Neuroendocrinology* **46**, 97–103
36. Urban, J. H., Das, I., and Levine, J. E. (1996) Steroid modulation of neuropeptide Y-induced luteinizing hormone releasing hormone release from median eminence fragments from male rats. *Neuroendocrinology* **63**, 112–119
37. Woller, M. J., and Terasawa, E. (1991) Infusion of neuropeptide Y into the stalk-median eminence stimulates in vivo release of luteinizing hormone-releasing hormone in gonadectomized rhesus monkeys. *Endocrinology* **128**, 1144–1150
38. Bristol-Gould, S. K., Kreeger, P. K., Selkirk, C. G., Kilen, S. M., Cook, R. W., Kipp, J. L., Shea, L. D., Mayo, K. E., and Woodruff, T. K. (2006) Postnatal regulation of germ cells by activin: the establishment of the initial follicle pool. *Dev. Biol.* **298**, 132–148
39. Knight, P. G., and Glistler, C. (2006) TGF- β superfamily members and ovarian follicle development. *Reproduction* **132**, 191–206
40. Pangas, S. A., Jorgez, C. J., Tran, M., Agno, J., Li, X., Brown, C. W., Kumar, T. R., and Matzuk, M. M. (2007) Intraovarian activins are required for female fertility. *Mol. Endocrinol.* **21**, 2458–2471
41. Murata, T., Takizawa, T., Funaba, M., Fujimura, H., Murata, E., Takahashi, M., and Torii, K. (1997) Quantitative RT-PCR for inhibin/activin subunits: measurements of rat hypothalamic and ovarian inhibin/activin subunit mRNAs during the estrous cycle. *Endocrine J.* **44**, 35–42
42. Xu, G., Zhong, Y., Munir, S., Yang, B. B., Tsang, B. K., and Peng, C. (2004) Nodal induces apoptosis and inhibits proliferation in human epithelial ovarian cancer cells via activin receptor-like kinase 7. *J. Clin. Endocrinol. Metab.* **89**, 5523–5534

43. Wang, H., Jiang, J.-Y., Zhu, C., Peng, C., and Tsang, B. K. (2006) Role and regulation of nodal/activin receptor-like kinase 7 signaling pathway in the control of ovarian follicular atresia. *Mol. Endocrinol.* **20**, 2469–2482
44. Cho, B. N., McMullen, M. L., Pei, L., Yates, C. J., and Mayo, K. E. (2001) Reproductive deficiencies in transgenic mice expressing the rat inhibin alpha-subunit gene. *Endocrinology* **142**, 4994–5004
45. Burger, L. L., Haisenleder, D. J., Wotton, G. M., Aylor, K. W., Dalkin, A. C., and Marshall, J. C. (2007) The regulation of FSH β transcription by gonadal steroids: testosterone and estradiol modulation of the activin intracellular signaling pathway. *Am. J. Physiol. Endocrinol. Metab.* **293**, E277–E285
46. Hoggard, N., Cruickshank, M., Moar, K. M., Barrett, P., Bashir, S., and Miller, J. D. B. (2009) Inhibin β B expression in murine adipose tissue and its regulation by leptin, insulin and dexamethasone. *J. Mol. Endocrinol.* **43**, 171–177
47. McGinnis, M. Y., Williams, G. W., and Lumia, A. R. (1996) Inhibition of male sex behavior by androgen receptor blockade in preoptic area or hypothalamus, but not amygdala or septum. *Physiol. Behav.* **60**, 783–789
48. Thackray, V. G., and Mellon, P. L. (2008) Synergistic induction of follicle-stimulating hormone β -subunit gene expression by gonadal steroid hormone receptors and Smad proteins. *Endocrinology* **149**, 1091–1102
49. Schwartz, M. W., Marks, J. L., Sipols, A. J., Baskin, D. G., Woods, S. C., Kahn, S. E., and Porte, D. (1991) Central insulin administration reduces neuropeptide Y mRNA expression in the arcuate nucleus of food-deprived lean (*Fa/Fa*) but not obese (*fa/fa*) Zucker rats. *Endocrinology* **128**, 2645–2647
50. Campbell, R. E., Ffrench-Mullen, J. M., Cowley, M. A., Smith, M. S., and Grove, K. L. (2001) Hypothalamic circuitry of neuropeptide Y regulation of neuroendocrine function and food intake via the Y5 receptor subtype. *Neuroendocrinology* **74**, 106–119
51. Li, C., Chen, P., and Smith, M. S. (1999) Morphological evidence for direct interaction between arcuate nucleus neuropeptide Y (NPY) neurons and gonadotropin-releasing hormone neurons and the possible involvement of NPY Y1 receptors. *Endocrinology* **140**, 5382–5390
52. Turi, G. F., Liposits, Z., Moenter, S. M., Fekete, C., and Hrabovszky, E. (2003) Origin of neuropeptide Y-containing afferents to gonadotropin-releasing hormone neurons in male mice. *Endocrinology* **144**, 4967–4974
53. Crowley, W. R., Hassid, A., and Kalra, S. P. (1987) Neuropeptide Y enhances the release of luteinizing hormone (LH) induced by LH-releasing hormone. *Endocrinology* **120**, 941–945
54. Broberger, C., de Lecea, L., Sutcliffe, J. G., and Hökfelt, T. (1998) Hypocretin/orexin- and melanin-concentrating hormone-expressing cells form distinct populations in the rodent lateral hypothalamus: relationship to the neuropeptide Y and agouti gene-related protein systems. *J. Comp. Neurol.* **402**, 460–474
55. Hahn, T. M., Breininger, J. F., Baskin, D. G., and Schwartz, M. W. (1998) Coexpression of *Agrp* and NPY in fasting-activated hypothalamic neurons. *Nat. Neurosci.* **1**, 271–272
56. Li, S., Hong, M., Fournier, A., St-Pierre, S., and Pelletier, G. (1994) Role of neuropeptide Y in the regulation of gonadotropin-releasing hormone gene expression in the rat preoptic area. *Brain Res. Mol. Brain Res.* **26**, 69–73
57. Xu, M., Hill, J. W., and Levine, J. E. (2000) Attenuation of luteinizing hormone surges in neuropeptide Y knockout mice. *Neuroendocrinology* **72**, 263–271
58. Bai, F. L., Yamano, M., Shiotani, Y., Emson, P. C., Smith, A. D., Powell, J. F., and Tohyama, M. (1985) An arcuate-paraventricular and -dorsomedial hypothalamic neuropeptide Y-containing system which lacks noradrenaline in the rat. *Brain Res.* **331**, 172–175
59. Shoji-Kasai, Y., Ageta, H., Hasegawa, Y., Tsuchida, K., Sugino, H., and Inokuchi, K. (2007) Activin increases the number of synaptic contacts and the length of dendritic spine necks by modulating spinal actin dynamics. *J. Cell Sci.* **120**, 3830–3837
60. Kupersmidt, L., Amit, T., Bar-Am, O., Youdim, M. B. H., and Blumenfeld, Z. (2007) The neuroprotective effect of activin A and B: implication for neurodegenerative diseases. *J. Neurochem.* **103**, 962–971
61. Goodarzi, M. O., Dumesic, D. A., Chazenbalk, G., and Azziz, R. (2011) Polycystic ovary syndrome: etiology, pathogenesis and diagnosis. *Nat. Rev. Endocrinol.* **7**, 219–231
62. Ewens, K. G., Stewart, D. R., Ankener, W., Urbanek, M., McAllister, J. M., Chen, C., Baig, K. M., Parker, S. C. J., Margulies, E. H., Legro, R. S., Dunaif, A., Strauss, J. F., and Spielman, R. S. (2010) Family-based analysis of candidate genes for polycystic ovary syndrome. *J. Clin. Endocrinol. Metab.* **95**, 2306–2315

Received for publication November 4, 2011.
Accepted for publication August 20, 2012.